Available online at www.sciencedirect.com
SCIENCE DIRECT®
Diamond and Related Materials 13 (2004) 1377–1384
DIAMOND AND RELATED MATERIALS
www.elsevier.com/locate/diamond

Incorporation of sulfur into hydrogenated amorphous carbon films

J. Filik[a], I.M. Lane[a], P.W. May[a,*], S.R.J. Pearce[a], K.R. Hallam[b]

[a]*School of Chemistry, University of Bristol, Cantock's Close, Bristol BS8 1TS, UK*
[b]*Interface Analysis Centre, University of Bristol, Oldbury House, 121 St. Michael's Hill, Bristol BS2 8BS, UK*

Abstract

Amorphous hydrogenated carbon–sulfur thin films (a-C:H:S) were deposited from CH_4/H_2S gas mixtures by capacitively-coupled radio-frequency PECVD. X-ray photoelectron spectroscopy (XPS) and secondary ion mass spectrometry (SIMS) were used to probe the composition of the films. XPS showed that the sulfur atomic percentage within a film was proportional to the fraction of H_2S in the H_2S/CH_4 gas mixture, and that films had been deposited with a sulfur content of up to 27 at.%. SIMS showed that the distribution of C and S was homogeneous throughout the films. Ex situ variable angle spectroscopic ellipsometry was used to evaluate the band gap energy variation by three different methods. Values of the E04 band gap for these films were between 1.5 and 2.5 eV, with refractive index values of between 1.8 and 2.1. Laser Raman spectroscopy (514.5 nm) suggested that the addition of sulfur increases the clustering of aromatic six-membered rings.

Keywords: Diamond-like carbon; Amorphous hydrogenated carbon; Amorphous alloys; Optical properties

1. Introduction

The fields of diamond-like carbon (DLC) and amorphous carbon (a-C) have been intensively studied [1,2] as a route to hard coatings or novel semiconductors. This is because these films can exhibit some of the extreme properties of diamond without requiring the harsh growth conditions traditionally employed for CVD diamond. Over the years, research has developed to include amorphous thin films that contain carbon and another element, such as nitrogen or phosphorus. Crystalline versions of these CN_x or CP_x compounds may have useful mechanical or electronic properties. For example, crystalline carbon nitride (C_3N_4) is predicted to be harder than diamond [3], although single crystal carbon nitride thin films have yet to be produced. Work has been reported previously by our group in Bristol using DLC deposition methods [4,5] to produce thin films of $C_xP_yH_z$, where the carbon content can be as low as 25%. The main objective of that work was to produce crystalline films of the (theoretically [6]) thermodynamically stable compound, phosphorus carbide (or carbon phosphide) C_3P_4, but so far, only amorphous $C_xP_yH_z$ films have been reported.

Similarly, if a sulfur-containing gas is added to the gas mixture during deposition instead of gases containing nitrogen or phosphorus, it may be possible to produce a solid material C_xS_y. Previous attempts to make such a material have used carbon disulfide (CS_2) as a convenient source of C and S, and thermal, plasma or catalytic activation to induce polymerisation. In 1868, Loew [7] observed that carbon disulfide produces a dark precipitate on exposure to sunlight, and in 1910 Dewar and Jones [8] added $CSCl_2$ to $Ni(CO)_4$ and produced a material that they concluded to be polymeric $(CS)_x$. The most important finding came when Bridgman [9] heated liquid carbon disulfide to 175 °C, at 45 kbar and produced a black solid that, on heating to 200 °C at atmospheric pressure, decomposed to carbon and sulfur. The electrical properties of a synthetically produced version of this black powder were studied by Tsukamoto and Takahashi [10], and it was found to have a band gap of 1.7 eV and a room temperature conductivity of $\sim 10^{-8}$ S cm^{-1}, which could be increased to $\sim 10^{-3}$ S cm^{-1} by n- or p-type doping with nitrogen or iodine, respectively. More recently, Spiro et al. [11] decomposed carbon disulfide in a hot filament reactor to produce films of approximate composition C_3S with electrical

*Corresponding author. Tel.: +44-117-928-9927; fax: +44-117-925-1295.
E-mail address: paul.may@bris.ac.uk (P.W. May).

0925-9635/04/$ - see front matter © 2003 Elsevier B.V. All rights reserved.
doi:10.1016/j.diamond.2003.08.026

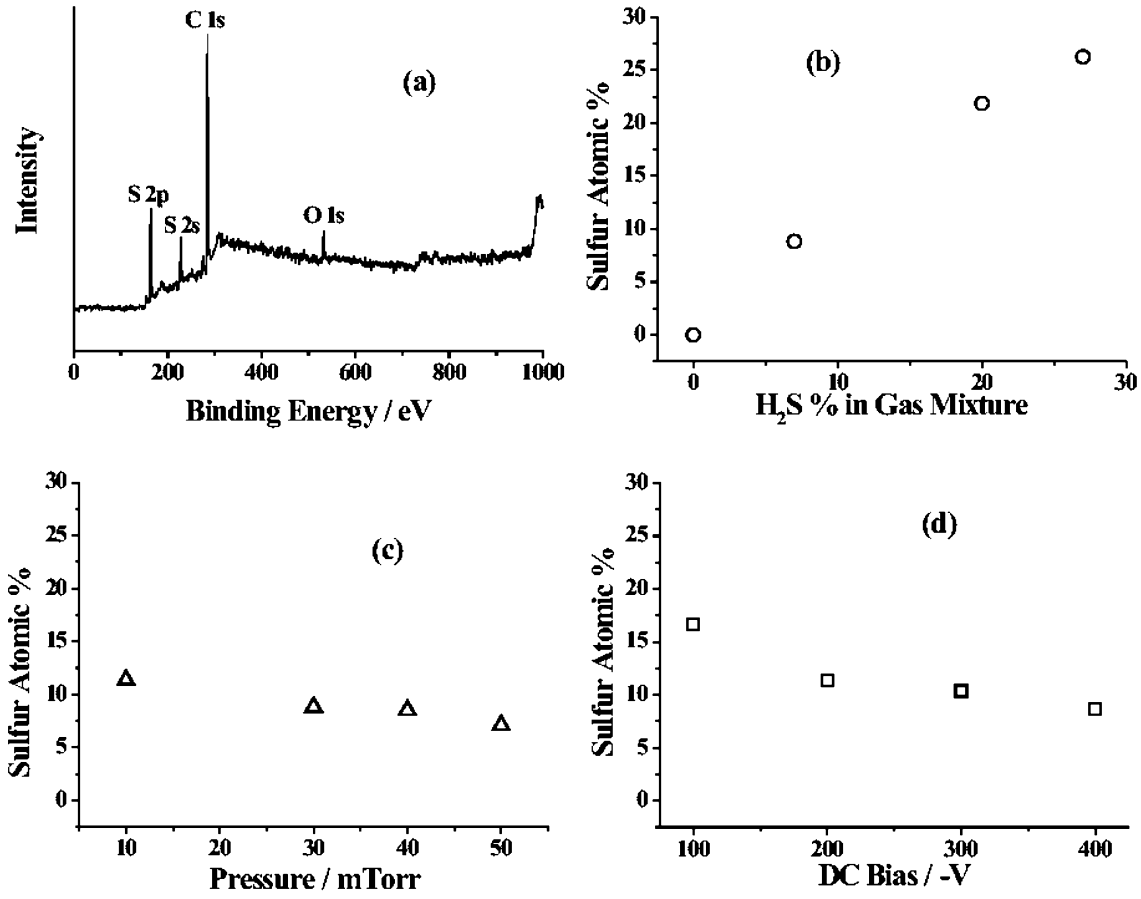

Fig. 1. XPS analysis: (a) A wide spectrum of an a-C:S:H film grown with a CH_4/H_2S ratio of 14:1, DC bias −100 V, pressure of 10 mTorr, with peaks labelled. Variation in surface sulfur content with (b) % H_2S in gas phase, (c) deposition pressure and (d) DC bias.

conductivity above $10^2\ \Omega^{-1}\,cm^{-1}$. Asano [12] produced carbon disulfide polymers by radio-frequency (RF) plasma-enhanced chemical vapour deposition (inductively- and capacitively-coupled) and found them to have similar values for refractive index and band gap as the polymer produced by Bridgman's method, but with a composition that was dependant on deposition conditions. Sadhir and Schoch [13] used (inductively-coupled RF) plasma-polymerised CS_2 as a cathode material for rechargeable batteries. A different approach was taken by Al-Dallal et al. [14], who produced hydrogenated amorphous carbon–sulfur alloys by decomposing 3.5% CH_4/H_2S in 96.5% Ar at 0.5 Torr in a capacitively-coupled RF reactor, as a follow up to their previous work on a-Si:S:H films [15].

However, despite their potential semiconductor applications, there has been very little systematic work to study the properties of thin films of C–S–H. Therefore, the aim of this present work is to make amorphous hydrogenated carbon–sulfur (a-C:S:H) thin films with a range of C:S ratios, and to study their electronic and mechanical properties.

2. Experimental

Films were deposited using a 13.56-MHz capacitively-coupled RF plasma reactor. Process gases of CH_4 and H_2S were controlled by mass flow controllers (maximum flow rates of 30 and 10 sccm, respectively) to give a total gas flow rate of between 10 and 35 sccm. A plasma was struck between two parallel-plate electrodes using an RF power supply. The upper electrode was grounded, and the RF power was applied to the lower electrode to produce a DC self-bias of between −100 and −400 V. The chamber pressure was maintained at between 10 and 50 mTorr. Substrates were ~1 cm^2 mirror-polished Si (1 0 0) wafers that were cleaned by sonification in isopropyl alcohol, dried and then washed with acetone, before being placed on the powered electrode. The deposition time was varied to produce different film thicknesses.

The film surface composition was determined by X-ray photoelectron spectroscopy (XPS), which allowed detection and quantification of all elements (except for hydrogen). A typical XPS spectrum of an a-C:S:H film

is shown in Fig. 1a. The relative fraction of each element present in the area analysed was derived from the individual peak areas since the associated sensitivity factors are known [16]. The variation of composition with depth was monitored by secondary ion mass spectrometry (SIMS) depth profiling.

Laser Raman spectroscopy (LRS) was used to study the structure of the carbon atoms in a film. 514 nm was the preferred laser wavelength used for LRS analysis of these films due to its sensitivity to sp^2 hybridised carbon ($\approx$50 times more sensitive than to sp^3 hybridised carbon). In general, two main peaks are seen in spectra taken from amorphous carbon films, the G peak and the D peak. The G peak is due to a bond stretching vibration of a pair of sp^2 sites [17] (chains or rings). The D peak is due to an A_{1g} breathing vibration of a sixfold aromatic ring that is activated by disorder [18]. For comparison of films, the ratio of the intensity of these peaks, $I(D)/I(G)$, is related to the size of any graphitic clusters present. The $I(D)/I(G)$ ratio was obtained by fitting the Raman spectra with two Gaussians, along with a quadratic base line to compensate for the photoluminescence background.

The optical properties and film thickness were determined by variable angle spectroscopic ellipsometry (VASE), over the range of 200–1000 nm at angles of 55, 60, 65, 70 and 75°. The Ψ and Δ values (which are parameters related to the change of the light polarization caused by its interaction with a sample) were then fitted using, as a model, a layer of amorphous semiconductor on 0.5-mm-thick crystalline Si. To describe the optical properties of the amorphous semiconductor layer, the Tauc–Lorentz model developed by Jellison and Modine [19] was used. This model has been shown [20] to evaluate the thickness and band gap of DLC films better than the Forouhi and Bloomer model [21] used previously. The parameters in the model were varied until the fitted spectrum matched the experimental data. From this fit, values of refractive index n, extinction coefficient k, film thickness and optical band gap were obtained. In order to facilitate comparison between our values and literature values (which often quote different versions of the band gap), the optical band gap was determined from the values of these parameters by three separate methods: Tauc–Lorentz fitting, Tauc extrapolation and the E04 method.

(a) The Tauc–Lorentz value for the band gap was a fitting parameter in Jellison and Modine's model and was determined by the values required to fit the ellipsometric parameters Ψ and Δ.

(b) The other two values for the band gap were obtained from the absorption coefficient, α, which was derived from the value of the extinction coefficient k ($=\alpha\lambda/4\pi$). By plotting a graph of $(E\alpha)^{1/2}$ as a function of energy, E, the intercept of the linear portion of the plot on the energy axis gave the Tauc [2] band gap.

(c) The E04 [2] band gap is the value of the energy E for which $\alpha = 10^4$.

3. Results

3.1. Composition, uniformity and structure

All a-C:H:S films were smooth, brightly coloured and slightly softer than the equivalent a-C:H films grown under similar conditions (established by the tendency of the films to get slightly scratched when handled with tweezers). The a-C:H:S films also showed less of a tendency to delaminate, and were electrically resistive beyond the limits that could be measured by four-point probe conductivity measurements.

Fig. 1a shows a typical wide XPS spectrum of an a-C:H:S film. The peaks are due to carbon 1s, sulfur 2s, sulfur 2p and oxygen 1s. The surface oxygen content is due to atmospheric oxidation and was seen to increase slightly with time between deposition and analysis. Fig. 1b–d show how the atomic percentage of S in the films varies with deposition conditions. The S content is directly proportional to the fraction of H_2S in the gas mixture from which the film was grown (Fig. 1b), and for higher H_2S flows the films have an S content over 27 at.%. The H content of the films was not measured, but from previous work on undoped a-C:H films using similar deposition conditions [22] it is expected that the H content will be approximately 2–7 at.%.

In Fig. 1c, the S content is shown to be inversely proportional to chamber pressure. This could possibly be due to the shorter mean free path at higher pressure causing more collisions in the plasma, encouraging the polymerisation of sulfur species. These polymers deposit in colder parts of the chamber, e.g. on the quartz window and by the pump inlet where there is no plasma. Such reactions could act as a sink for the S species, reducing the availability of S for film growth.

Fig. 1d shows that the S content is inversely proportional to the DC bias. It has previously been observed that the H content of a-C:H films also varies in this manner [23]. For hydrogen, the increase in ion impact energy causes increased displacement of H atoms within the film. The H-displaced atoms can either remain trapped, or they can form H_2 by recombination with another H atom or by H abstraction from the a-C:H film. The H_2 molecules can also remain trapped in voids, or they may diffuse to the surface, in which case they will emerge back into the gas phase, thereby reducing the overall H content of the film. Also, the higher power required to produce a higher bias increases the dissociation of the molecules in the plasma; this may increase the concentration of H ions/radicals at the

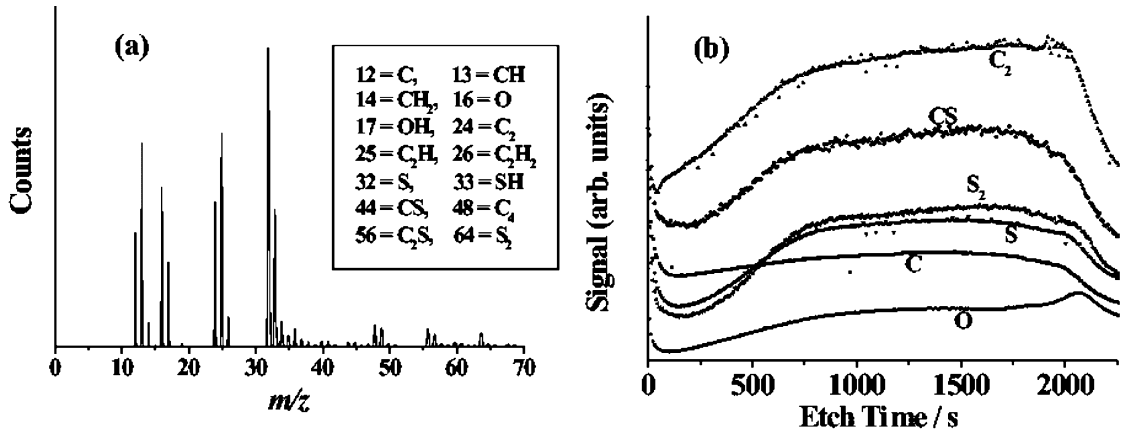

Fig. 2. (a) SIMS spectrum of an a-C:S:H film, growth conditions as in Fig. 1a. (b) A SIMS depth profile of the same film.

growing film surface leading to chemical etching of any surface-bound H. The same physical and chemical sputtering/etching arguments may be applied to the behaviour of sulfur as a function of bias in the a-C:S:H films. This mechanism fits well with the observations from Al-Dallal et al. [14] who attributed low temperature (~200 °C) gas evolution of H_2S to the release of void-trapped H_2S, as opposed to H_2S from the rupture of C–S bonds.

Fig. 2a shows a SIMS spectrum from an a-C:H:S film. Unsurprisingly, the largest peaks are due to small ions containing C, S and/or H. However, the data from SIMS must be interpreted with care. SIMS data are not quantitative, so the relative intensities of the peaks cannot be compared in order to calculate the relative abundances. The depth profile of the same a-C:S:H film is shown in Fig. 2b. At the start of the depth profile (0–500 s) the etch rate of the ions takes time to equilibrate, so this section is not an accurate description of the film composition. Between 500 and 2000 s the profile is flat suggesting a homogeneous composition of the monitored species within the film. At approximately 2100 s there is a peak in the oxygen trace that corresponds to the depth profile reaching the native oxide layer on the Si substrate.

The laser Raman spectra shown in Fig. 3a show that the D peak intensity (at the position shown by the arrow) gradually increases with increasing H_2S in the gas phase. This suggests that the presence of S in the film, or its effect on the plasma chemistry, increases the aromatic six-membered ring clustering within the film. This can also be seen by plotting the $I(D)/I(G)$ ratio against the deconvoluted G peak width for all the films grown. Both $I(D)/I(G)$ and the G linewidth are proportional to the cluster size [24] (Fig. 3b), so a reasonably straight line is produced which reflects the increase in

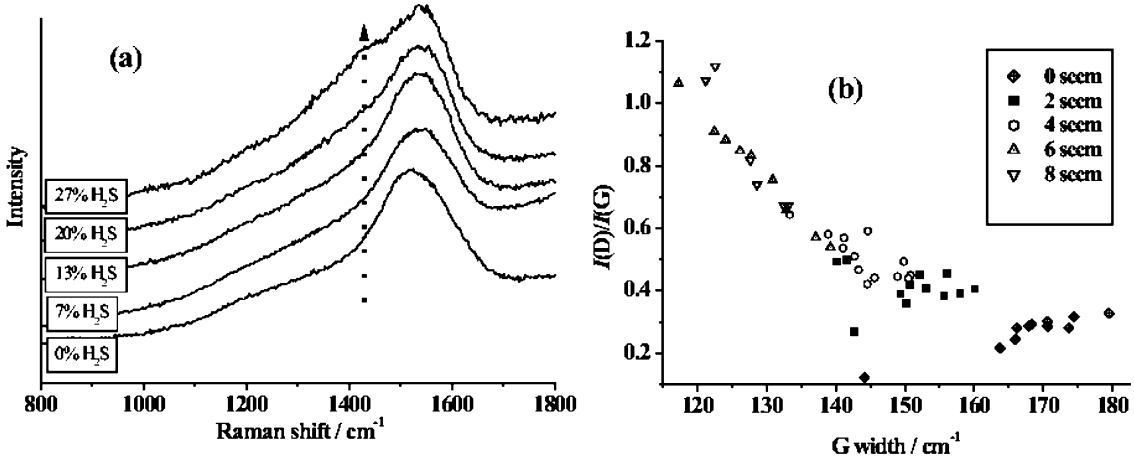

Fig. 3. (a) Laser Raman spectra of various a-C:S:H films grown with increasing H_2S content in the gas phase, showing the evolution of the D peak at the position indicated by the dotted arrow. These spectra have been offset vertically for clarity. (b) A plot of $I(D)/I(G)$ ratio vs. G peak width for different flows of H_2S (total gas flow rate constant at 30 sccm).

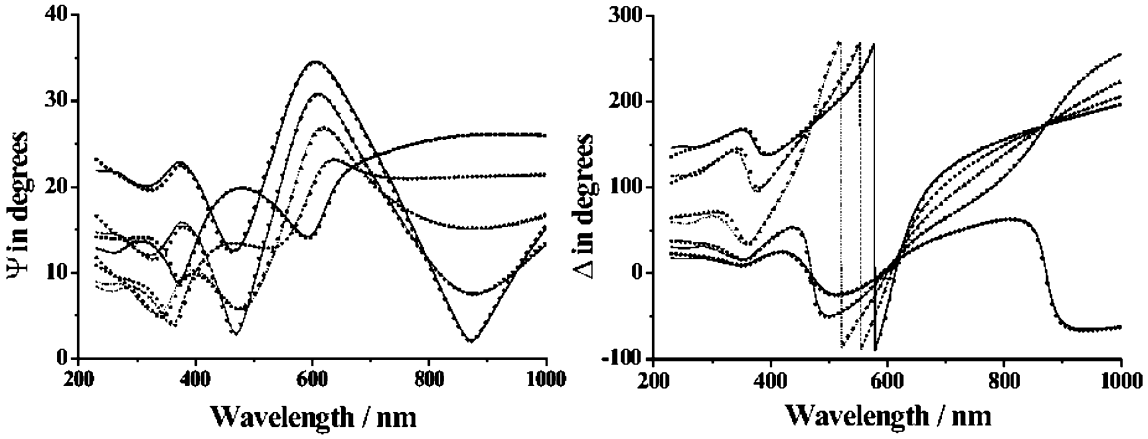

Fig. 4. Ellipsometry spectra demonstrating the accuracy of the ellipsometry fitting using Jellison and Modine's model [19] to the Ψ (left) and Δ (right) values from VASE. Experimental data are shown as lines and the fitted spectra as dots.

clustering as the flow of H_2S is increased from 0 to 8 sccm (out of a total gas flow rate of 30 sccm), which corresponds to 0–27% H_2S in the gas phase.

3.2. Growth rate and optical properties

The quality of the fitted ellipsometry data produced

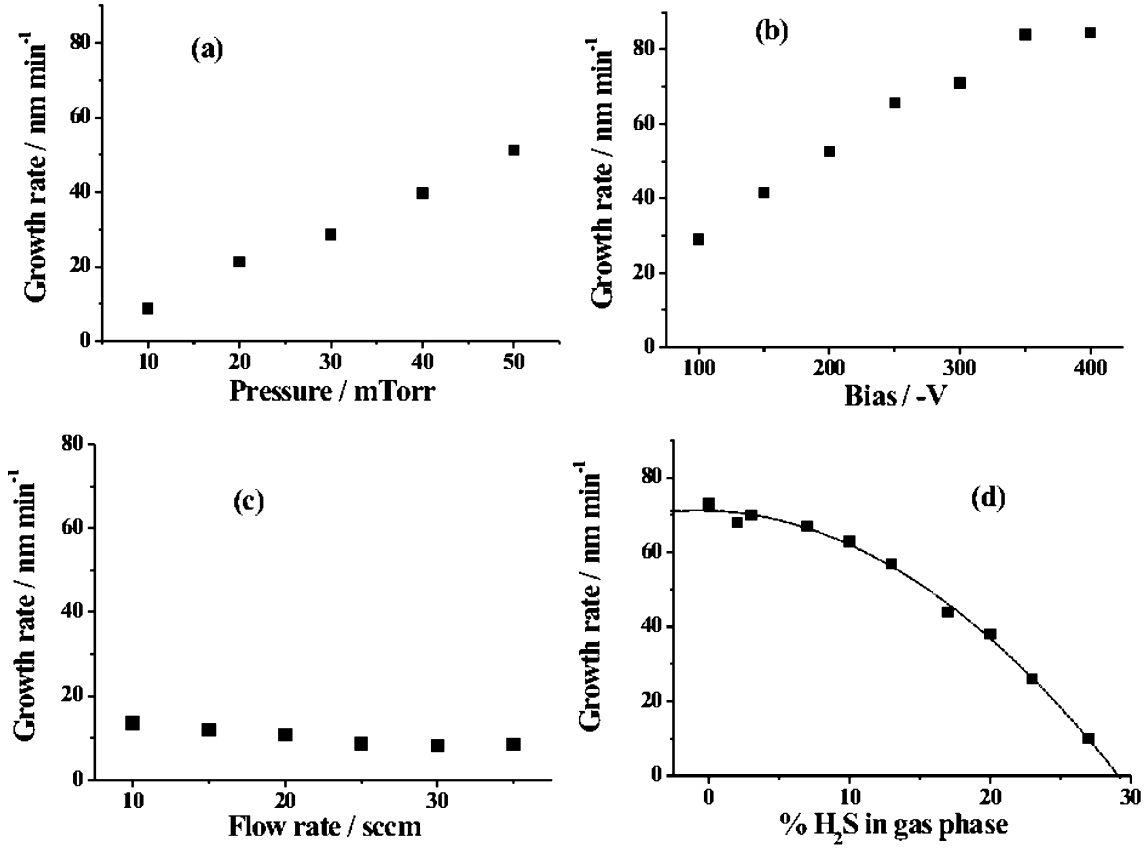

Fig. 5. Variation of growth rate with deposition conditions: (a) chamber pressure (DC bias = −100 V, 6.7% H_2S in the H_2S/CH_4 gas mixture, total gas flow rate = 30 sccm); (b) DC bias (pressure = 30 mTorr, 6.7% H_2S in the H_2S/CH_4 gas mixture, total gas flow rate = 30 sccm); (c) total gas flow rate (DC bias = −100 V, pressure = 10 mTorr, 6.7% H_2S in the H_2S/CH_4 gas mixture) and (d) % H_2S in gas phase (DC bias = −200 V, pressure = 30 mTorr, total gas flow rate = 30 sccm). In (d), the data have been fitted to a quadratic function, shown as a dotted line.

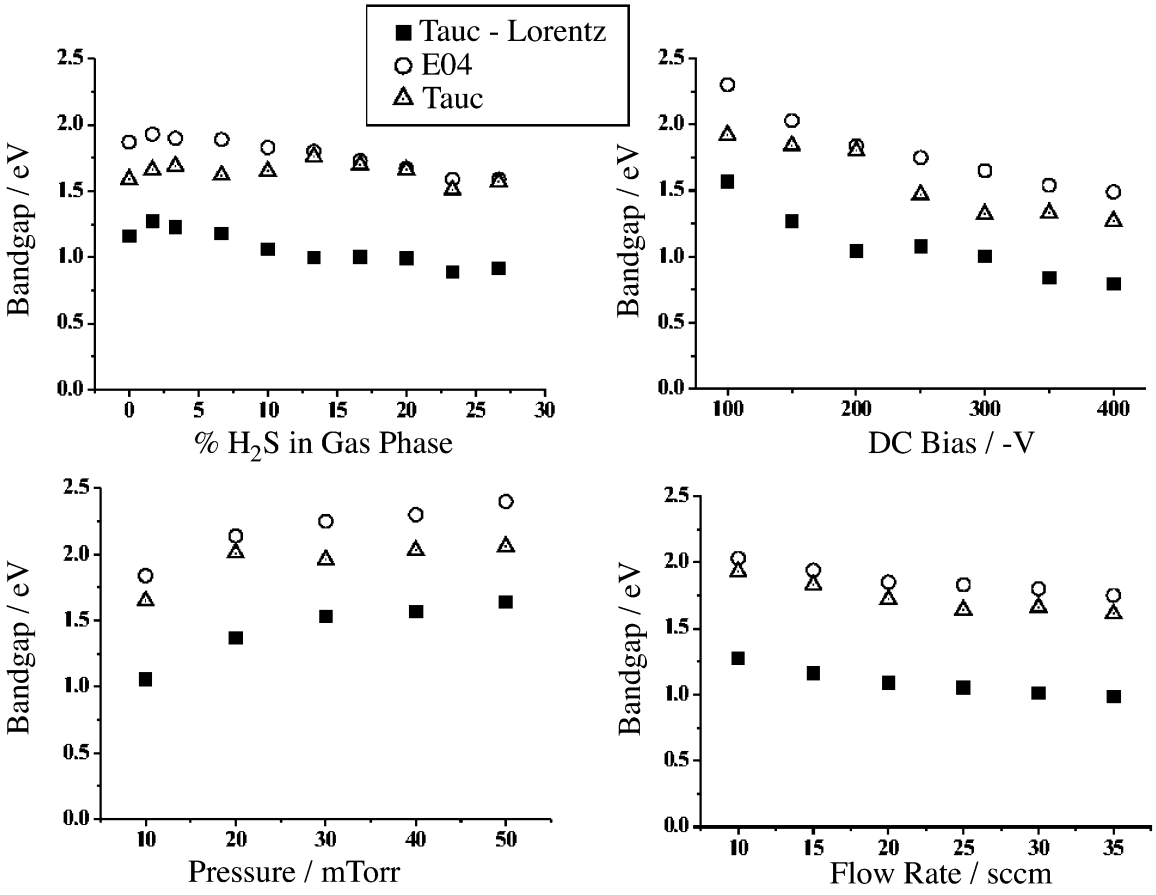

Fig. 6. Variation of the three versions of the band gap with deposition conditions, all other conditions as in Fig. 5.

by the Tauc–Lorentz model is shown in Fig. 4. Attempts were made to improve the fit by using interfacial or roughness layers but neither significantly improved on the simple amorphous semiconductor on crystalline silicon model.

Fig. 5a–d show the variation in the film growth rate (estimated from ellipsometry) with deposition conditions. The function of growth rate against chamber pressure (a) appears to be linear, as does the growth rate with DC bias (b) for smaller values (−100 to −300 V). As the bias is increased above this, the growth rate levels off, possibly due to the sputtering rate increasing with the higher energy ion impacts. The total gas flow rate (c) has only a relatively small effect on the growth rate (over the range of the 50-sccm mass flow controller) compared to other conditions. The most interesting result is the variation with the percentage of H_2S in the gas phase (d). The data can be fitted approximately with a quadratic curve, showing that the decrease in growth rate is not simply caused by the linear decrease in carbon-containing species. If the H_2S/CH_4 ratio becomes too high, no film is deposited (growth rate is 0). This is surprising, since there are still carbon species in the plasma, so a-C:H deposition should still be occurring. To account for this, we suggest that S-containing species within the plasma, in high enough concentrations, are able to etch the growing a-C:S:H film by producing neutral volatile molecules on the film surface, such as CS_2, CH_3SH, etc., which then desorb and are pumped away. Thus, there is a competition between deposition and etching. In carbon-rich gas mixtures, deposition dominates and the S is incorporated into the growing film by implantation and/or chemical means. For S-rich gas mixtures, etching dominates and no films are deposited.

Fig. 6 shows the variation of the three different measurements of the optical band gap (Tauc, E04 and the Tauc–Lorentz) as a function of the deposition conditions. The amount of sulfur in the gas phase (or the film) causes the optical band gap to vary by ~0.4 eV, compared to the ~0.8 eV shift caused by the DC bias. The band gap is seen to increase from 1.59 to 1.66 eV (E04) when the H_2S gas phase proportion is increased from 0 to 1.67%. This has also been observed [25] with the addition of nitrogen to a-C:H films, where it is believed to be due to initially incorporated N acting as passivator of the dangling bond states. The decrease in band gap with increasing S could reflect the increase

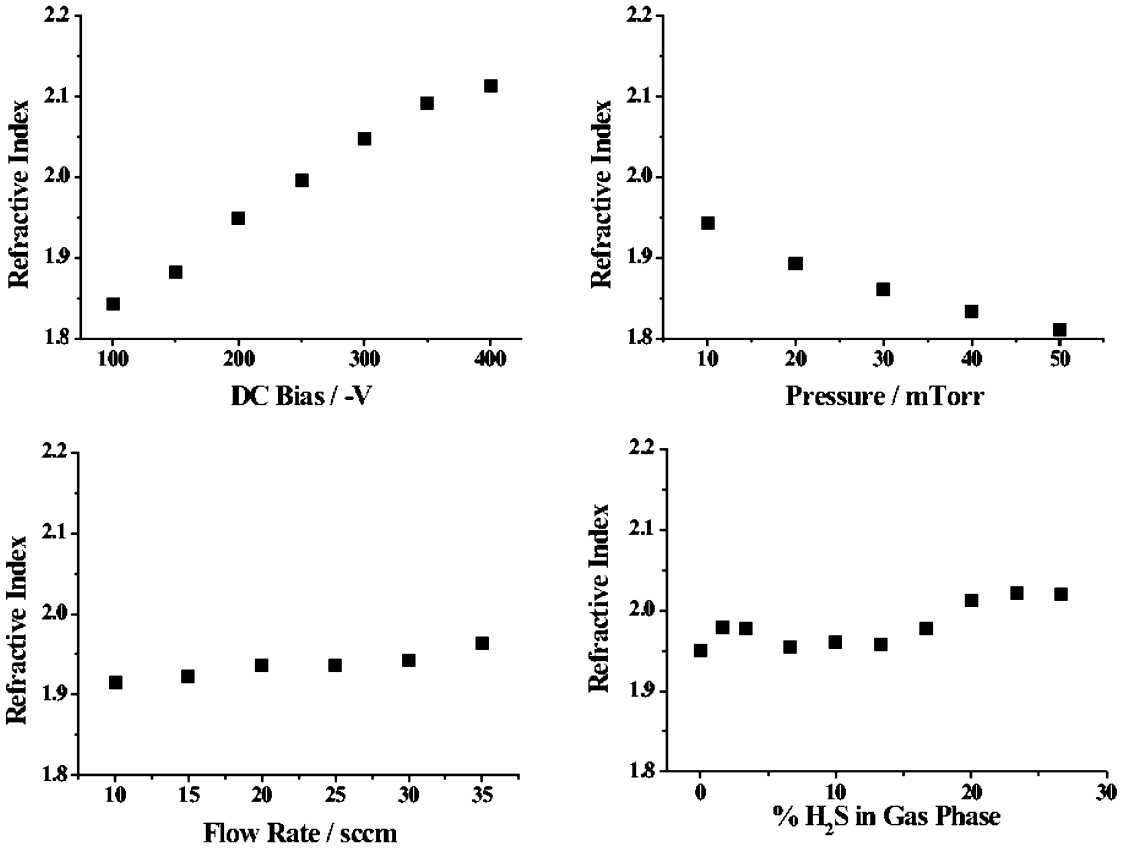

Fig. 7. Variation of refractive index with deposition conditions, all other conditions as in Fig. 5.

in the graphitic ring clustering seen in the Raman spectra.

The variation with deposition conditions of the refractive index, n, at 675.8 nm (obtained by spectroscopic ellipsometry) is shown in Fig. 7. The refractive index has been shown to correlate with hardness and resistance to laser damage [26]. Diamond-like a-C:H films tend to have refractive indices between 1.6 and 2.3, and if $n<1.6$ the films are designated more 'polymer-like' than diamond-like. Fig. 6 shows that since $n>1.8$ for all of these films, we conclude that the bonding in the a-C:S:H films is still predominantly diamond-like. The DC bias and pressure have a far greater effect (over the range studied) on n than the S content. Changing the bias increased n by ~ 0.25, compared to a variation of only ~ 0.07 on going from 0 to $\sim 27\%$ S.

4. Conclusions

We have shown that for a CH_4/H_2S gas mixture containing 27% H_2S, films can be deposited that contained approximately 27% S. We have also seen that the S is distributed homogeneously throughout the film, and that this does not have a particularly large effect on the refractive index. The band gap of the films can be tuned by 0.4 eV by changing the gas phase H_2S content, but the Raman $I(D)/I(G)$ ratio suggests that this may be due to an increase in the clustering of sixfold aromatic rings. To produce films similar to the polymeric $(CS_2)_x$ reported by Sadhir and Schoch [13] would require 66% H_2S in the gas phase, but with this composition the growth rate using the present method would be extremely slow, if not zero. The films we have produced have a similar S:C ratio as the films grown from hot filament activated CS_2/Ar mixture in Ref. [11] but with different electrical properties. This could be due to the presence of hydrogen in our films, suggesting that it might be rewarding to deposit films from CS_2 or CS_2/Ar plasmas.

References

[1] J. Roberson, Mater. Sci. Eng. R 37 (2002) 129.
[2] S.R.P. Silva, J.D. Carey, R.U.A. Khan, E.G. Gerstner, J.V. Anguita, in: H.S. Nalwa (Ed.), Amorphous Carbon Thin Films, vol. 4, Handbook of Thin Film Materials, Academic Press, 2002, pp. 403–505, Chapter 9.
[3] S. Muhl, J.M. Mendez, Diamond Relat. Mater. 8 (1999) 1809.
[4] S.R.J. Pearce, P.W. May, R.K. Wild, K.R. Hallam, P.J. Heard, Diamond Relat. Mater. 11 (2002) 1422.
[5] S.R.J. Pearce, J. Filik, P.W. May, R.K. Wild, K.R. Hallam, P.J. Heard, Diamond Relat. Mater. 12 (2003) 979.
[6] F. Claeyssens, N.L. Allan, P.W. May, P. Ordejon, J.P. Oliva, Chem. Commun. 2 (2002) 2494.
[7] O. Loew, Z. Chem. 4 (1868) 622.

[8] J. Dewar, H.O. Jones, Proc. R. Soc. Lond., A 83 (1910) 408.
[9] P.W. Bridgman, J. Appl. Phys. 12 (1941) 461.
[10] J. Tsukamoto, A. Takahashi, Jap. J. Appl. Phys. 25 (1986) L338.
[11] C.L. Spiro, W.F. Banholzer, D.S. McAtee, Thin Solid Films 220 (1992) 122.
[12] Y. Asano, Jap. J. Appl. Phys. 22 (1983) 1618.
[13] R.K. Sadhir, K.F. Schoch Jr., Chem. Mater. 8 (1996) 1281.
[14] S. Al-Dallal, S.M. Al-Alawi, S. Aljishi, M. Hamman, S. Arekat, J. Non-Cryst. Solids 196 (1996) 168.
[15] S. Al-Dallal, M. Hammam, S.M. Al-Alawi, S. Alijishi, A. Breitschwardt, Philos. Mag. B 63 (1992) 211.
[16] J. Chastain (Ed.), Handbook of X-ray Photoelectron Spectroscopy, Perkin-Elmer Corp, 1992.
[17] A.C. Ferrari, J. Robertson, Phys. Rev. B. 61 (2000) 14095.
[18] F. Tuinstra, J.L. Koenig, J. Chem. Phys. 53 (1970) 1126.
[19] G.E Jellison Jr., F.A. Modine, Appl. Phys. Lett. 69 (1996) 371.
[20] J. Hong, A. Goullet, G. Turban, Thin Solid Films 352 (1999) 41.
[21] A.R. Forouhi, I. Bloomer, Phys. Rev. B 34 (1986) 7018.
[22] J. Filik, P.W. May, S.R.J. Pearce, R.K. Wild, K.R. Hallam, Diamond Relat. Mater. 12 (2003) 974.
[23] A. von Keudal, W. Jacob, in: S.R.P Silva (Ed.), Properties of Amorphous Carbon, INSPEC, London, 2001, Chapter 9.2.
[24] J. Schwan, S. Ulrich, V. Batori, H. Ehrhardt, S.R.P. Silva, J. Appl. Phys. 80 (1996) 440.
[25] S.R.P. Silva, G.A.J. Amaratunga, Thin Solid Films 270 (1995) 194.
[26] D.P. Dowling, K. Donnelly, M. Monclus, M. McGuinness, Diamond Relat. Mater. 7 (1998) 432.